Int. J. Heat Mass Transfer. Vol. 34, No. 12, pp. 3135–3142, 1991
Printed in Great Britain

0017–9310/91 $3.00+0.00

Convective–radiative heat transfer in the thermal entrance region of the semicircular duct with streamwise internal fins

H. Y. ZHANG and M. A. EBADIAN
Department of Mechanical Engineering, Florida International University, Miami, FL 33199, U.S.A.

(*Received* 27 *August* 1990 *and in final form* 3 *December* 1990)

Abstract—In this paper, steady laminar forced convection and radiation heat transfer in the entrance region of an internally finned semicircular duct are analyzed. The fins are continuous and longitudinal, with zero thickness. The thermal condition imposed on the semicircular duct is of uniform temperature, both axially and peripherally. The three-dimensional energy equation is discretized and solved numerically by the method of lines (MOL). The method of momentum (MOM) is employed to consider the radiation contribution, which models the radiation in the partial differential equation, instead of the partial integro-differential equation. The resulting equations, based on coarse grids, are numerically computed, using a Runge–Kutta subroutine. The effect of five major parameters on the thermal behavior in the entry region of the semicircular duct is discussed: radiation–conduction, N; optical thickness, τ_b; wall emissivity, ε_w; number of fins, M; and ratio of fin height to duct radius, H. The variations in the mean bulk temperature and total Nusselt numbers show that heat transfer is enhanced in this geometry by both thermal radiation and fins.

INTRODUCTION

RADIATION–convection interaction problems with internal fins are found when considering the cooling of high temperature components and furnace design in which heat transfer occurs by parallel radiation and convection.

This study deals with the analytical/numerical solution of combined radiation and convection in the thermal entry region of the semicircular duct with internal fins subjected to a uniform wall temperature (Fig. 1). A survey of literature by Eckert *et al.* [1–3], Kakac *et al.* [4], Shah and London [5], Soloukhin and Martynenko [6], and Martynenko [7], indicates that significant attention has been devoted in recent years to the investigation of combined radiation and laminar forced convection in a duct of circular or non-circular geometry. However, these investigations, along with Pearce and Emery [8], Echigo *et al.* [9], Yener and Fong [10], Hu and Chang [11], Nandakumar and Masliyah [12], Soliman and Feingold [13, 14], Soliman *et al.* [15], Prakash and Patankar [16], Prakash and Liu [17], and Rustum and Soliman [18, 19], have been restricted to situations that either do not account for internal fins, or the simultaneous effects of forced convection and radiation in the thermal entrance region of ducts where the flowing medium is a participating gas. One study related to the present problem, but restricted to a circular pipe under isothermal wall conditions, was carried out by Campo [20]. Various methods have been applied by this investigation to consider the cases of longitudinal fins for both steady-state and transient conditions. The Ritz method is applied in the steady-state case, while the Kantorovich method is applied to obtain the transient solution, assuming that the fin temperature profile is the product of a polynomial in position and an unknown function of time. The form of the polynomial position is evaluated from the steady-state condition. Comparison with numerical solutions shows good accuracy. Accordingly, in this type of problem, the energy and radiation transport equations must be solved simultaneously in order to determine the temperature profiles and heat transfer rates.

The radiative contribution in the present paper has been modeled by the method of moments (MOM) in two-dimensions, wherein the radiative transfer equation (RTE) is expressed in differential form [21]. The salient feature of this approach is that the RTE accounting for gray gas behavior is of an elliptic type, and consequently, may be accommodated into a general diffusion–convection type of equation. This approach also provides an additional conservation equation for irradiation.

In light of the foregoing, the resulting system of four partial differential equations is amenable to numerical analysis by employing the method of lines (MOL) [22]. According to this method, the transversal derivatives are replaced by finite difference formulations, and correspondingly, the region of integration is divided into a collection of lines parallel to the axial coordinate. It is widely known that the retention of equal transversal intervals in the presence of irregular boundaries constitutes a complicating feature requiring special equations for nodes in its neighborhood [23]. To prevent this complication and difficulty, a two-dimensional grid in the cross-stream direction is constructed in such a manner that the dividing lines

NOMENCLATURE

A	cross sectional area [m^2]
C	factor defined by equation (12)
C_p	specific heat [J kg^{-1} K^{-1}]
D_h	hydraulic diameter of duct [m]
f	friction factor
G	total irradiation [W m^{-2}]
G^*	dimensionless value of G, equation (9)
H	relative height of fin, L/r_i
k	thermal conductivity of fluid [W m^{-1} K^{-1}]
L	characteristic length of the duct, r_i [m]
M	number of fins
$\dot{m}$	mass flow rate of fluid [kg s^{-1}]
N	radiation–conduction parameter, equation (9)
Nu_T	total Nusselt number, equation (21)
$Nu_{m,T}$	mean Nusselt number, equation (22)
P	perimeter [m]
p	pressure [kN m^{-2}]
Pe	Peclet number, $Re\ Pr$
Pr	Prandtl number, ν/α
q_w	wall heat flux [W m^{-2}]
R	dimensionless variable, r/r_i
r	radial coordinate
Re	Reynolds number, $\bar{u}D_h/\nu$
T	temperature [K]
u, U	dimensional and dimensionless velocity of fluid, $u/\bar{u}$
$\bar{u}$, $\bar{U}$	dimensional and dimensionless mean velocity of fluid
w	generalized dependent variable
X	dimensionless axial coordinates, $(D_h^2/a^2)x^*$
x, x^*	dimensional and dimensionless axial coordinate, $x^* = x/(D_h\ Pe)$.

Greek symbols

α	thermal diffusivity of fluid [m^2 s^{-1}]
β	extinction coefficient [m^{-1}]
ε_w	wall emissivity
θ	angular coordinate
κ	volumetric absorption coefficient [m^{-1}]
λ_w	function, equation (16)
μ	dynamic viscosity of fluid [kg m^{-1} s^{-1}]
ν	kinematic viscosity of fluid [m^2 s^{-1}]
ρ	density of fluid [kg m^{-3}]
σ	Stefan–Boltzmann constant [W m^{-2} K^{-4}]
τ_h	optical thickness, equation (9)
ϕ	dimensionless temperature.

Subscripts

b	mean bulk
c	conduction
e	entrance
R	radiation
ref	reference
T	total
w	wall (circumferential).

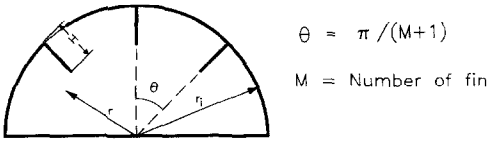

FIG. 1. Coordinate system for semicircular duct.

coincide with the irregular boundaries, resulting in equal or unequal transversal intervals. The partial differential equations are replaced by a system of ordinary differential equations of the first order (the independent variable is the axial coordinate), coupled to a system of algebraic equations. In the former, the temperature is the dependent variable, while in the latter, irradiation is the dependent variable. The numerical solution of this non-linear system may be readily obtained using Runge–Kutta and TDMA-like algorithms.

In this paper, the hybrid methodology (MOL) has been tested for ducts of semicircular cross section with longitudinal fins for several different geometries. The test is for three and seven fins within the semicircular duct, each with a relative fin height of 0.3 and 0.6, respectively. The solutions have been obtained in terms of the distribution of the mean bulk temperature and the total Nusselt number. The computed results, in the absence of radiation, are compared with ref. [24] and excellent agreement is observed.

It is believed that the availability of such hybrid solutions is important for the analysis and design of high temperature heat exchangers having ducts with semicircular cross sections and streamwise internal fins.

STATEMENT OF THE PROBLEM

The problem to be investigated is that of fully developed laminar combined radiation and forced convection through the internally finned, semicircular duct as shown schematically in Fig. 1. The fins are straight, continuous, and distributed equally around the tube circumference. The thickness of the fins is negligible. A uniform temperature prevails at all points on the fins and the semicircular duct wall. The fluid properties are constant. The participating gas is gray, emitting, absorbing, and nonscattering. Viscous dissipation, heat conduction and radiation in the axial

direction are negligible. Finally, the pressure gradient is the only function of the axial direction.

Governing equations

Under the foregoing assumptions, the equations governing the problem are:

Momentum equation.

$$\frac{1}{r}\frac{\partial}{\partial r}\left(r\frac{\partial u}{\partial r}\right)+\frac{1}{r^2}\frac{\partial^2 u}{\partial \theta^2}=\frac{1}{\mu}\frac{\mathrm{d}P}{\mathrm{d}x} \tag{1}$$

where x, r, and θ are the axial, radial, and angular coordinates of the duct, respectively. Additionally, μ is the dynamic viscosity and $\mathrm{d}P/\mathrm{d}X$ the pressure gradient in the axial direction. Equation (1) can be written in dimensionless form as

$$\frac{\partial^2 u^*}{\partial R^2}+\frac{1}{R}\frac{\partial u^*}{\partial R}+\frac{1}{R^2}\frac{\partial^2 u^*}{\partial \theta^2}+1=0 \tag{2}$$

where

$$u^*=\left\{\frac{r_i^2(-\mathrm{d}P/\mathrm{d}x)}{\mu}\right\}u,\quad R=\frac{r}{r_i}. \tag{3}$$

The boundary conditions are:

$$u^*=0 \quad @ \quad R=1$$

$$(1-H)\leqslant R\leqslant 1,\quad \theta=\frac{\pi}{(M+1)}$$

$$0\leqslant R\leqslant 1,\qquad \theta=0,\quad \pi \tag{4}$$

and

$$\frac{\partial u^*}{\partial \theta}=0 \quad @ \quad 0\leqslant R\leqslant (1-H),$$

$$\theta=\frac{\pi}{2}\text{ (for odd number of fins)} \tag{5}$$

where the definitions for the pressure gradient, $\mathrm{d}P/\mathrm{d}X$, and the hydraulic diameter are the same as those given in ref. [24].

The energy equation.

$$\rho c_p u\frac{\partial T}{\partial X}=k\left(\frac{\partial^2 T}{\partial r^2}+\frac{1}{r}\frac{\partial T}{\partial r}+\frac{1}{r^2}\frac{\partial^2 T}{\partial \theta^2}\right)$$

$$+\kappa(G-4\sigma T^4). \tag{6}$$

The second term on the right-hand side of equation (6) corresponds to thermal radiation, where κ is the total volumetric absorption coefficient, σ the Stefan–Boltzmann constant and irradiation, G, is given by

$$\frac{\partial^2 G}{\partial r^2}+\frac{1}{r}\frac{\partial G}{\partial r}+\frac{1}{r^2}\frac{\partial^2 G}{\partial \theta^2}=3\beta\kappa(G-4\sigma T^4) \tag{7}$$

where β in equation (7) represents the extinction coefficient for a non-scattering gas

$$\beta=\kappa. \tag{8}$$

By introducing the following dimensionless variables and parameters:

$$U=\frac{u}{\bar{u}},\quad \phi=\frac{T}{T_w}$$

$$R=\frac{r}{r_i},\quad D_h=\frac{\pi D^2}{(\pi+2)D+4MH}$$

$$X=\frac{D_h^2}{r_i^2}\frac{x}{D_h\,Pe},\quad Re=\frac{\bar{u}D_h}{\nu},\quad Pe=Re\,Pr$$

$$N=\frac{4\sigma T_w^3}{k\kappa},\quad \tau_b=\kappa a,\quad G^*=\frac{G}{4\sigma T_w^4}. \tag{9}$$

Energy equations (6) and (7) can be written in dimensionless form as

$$\frac{\partial\phi}{\partial X}=C\left[\frac{\partial^2\phi}{\partial R^2}+\frac{1}{R}\frac{\partial\phi}{\partial R}+\frac{1}{R^2}\frac{\partial^2\phi}{\partial\theta^2}\right]$$

$$+CN\tau_b^2(G^*-\phi^4) \tag{10}$$

and

$$\frac{\partial^2 G^*}{\partial R^2}+\frac{1}{R}\frac{\partial G^*}{\partial R}+\frac{1}{R^2}\frac{\partial^2 G^*}{\partial\theta^2}=3\tau_b^2(G^*-\phi^4) \tag{11}$$

where

$$C=\frac{D_h^4}{2r_i^4u^*(f\,Re)}. \tag{12}$$

The applicable boundary conditions for equation (10) are

$$\phi=1 \quad @ \quad R=1,\qquad 0\leqslant\theta\leqslant\pi$$

$$(1-H)\leqslant R\leqslant 1,\quad \theta=\frac{\pi}{(M+1)}$$

$$0\leqslant R\leqslant 1,\qquad \theta=0,\quad \pi \tag{13}$$

and

$$\frac{\partial\phi}{\partial\theta}=0 \quad @ \quad 0<R<(1-H),\quad \theta=\frac{\pi}{2}$$

and at the entrance region ($X=0$), $\phi(R,\theta,0)=\phi_e$.

The irradiation equation (11) is also subjected to the following boundary conditions:

$$\frac{\partial G^*}{\partial R}=-\tfrac{3}{2}\lambda_w\tau_b(G_w^*-1) \tag{14}$$

$$@ \quad R=1,\qquad 0<\theta<\pi$$

$$@ \quad (1-H)\leqslant R\leqslant 1,\quad \theta=\frac{\pi}{M+1}$$

$$@ \quad 0\leqslant R\leqslant 1,\qquad \theta=0,\quad \pi. \tag{15}$$

Also

$$\frac{\partial G^*}{\partial\theta}=0 \quad @ \quad 0<R<(1-H),\quad \theta=\frac{\pi}{2}$$

where in equation (14)

$$\lambda_w=\frac{\varepsilon_w}{2-\varepsilon_w} \tag{16}$$

and ε_w is the emissivity of the wall.

EXPRESSIONS FOR THE COMBINED NUSSELT NUMBER

The thermal characteristics of fluid flow inside any duct may be represented by the dimensionless bulk temperature as

$$\phi_b = \int_A U\phi \, dA \Big/ \int_A U \, dA. \tag{17}$$

In the case of combining convective and radiative heat transfer, the total Nusselt number is related to the total heat flux through the wall

$$Nu_T = \frac{q_w D_h}{k(T_w - T_b)} \tag{18}$$

where

$$q_w = q_{wc} + q_{wR}.$$

Here, q_{wc} and q_{wR} represent the contributions of convective and radiative heat transfer, respectively. There are two ways to determine q_w. One way is to calculate directly the heat flux in terms of the total and mean Nusselt numbers as follows:

$$Nu_T = \frac{\left[2\left.\frac{\partial\phi}{\partial n}\right|_w - 4N\lambda_w(G_w^* - 1)\right]}{1 - \phi_b} \tag{19}$$

$$Nu_{m,T} = \frac{\int Nu_T \, dX}{\int dX}. \tag{20}$$

Nu_T and $Nu_{m,T}$ can also be calculated by considering the first law of thermodynamics. Since heat transfer in the duct wall between two axial locations is equal to the energy change in the two cross sections [25]

$$Nu_T = \frac{1}{4\phi_b}\frac{d\phi_b}{dX} \tag{21}$$

and

$$Nu_{m,T} = \frac{1}{4X}\ln(\phi_b). \tag{22}$$

Equations (19) and (22) are used in computing the total Nusselt number.

NUMERICAL PROCEDURE

A numerical method is necessary to solve the nonlinear problem under consideration. Accordingly, the system of equations (10) and (11), subject to the boundary conditions expressed by equations (13)–(16) is numerically solved by combining the MOL and the fourth-order Runge–Kutta algorithm.

The temperature distribution, $\phi(R, \theta, X)$, has been determined by the hybrid MOL using uniform grids. The MOL has been described by Liskovets [22] as a solution technique that transforms a partial differential equation into an appropriate system of ordinary differential equations for a parabolic PDE involving three independent variables, as in equation (10). The region of integration may be divided into lines parallel to the axial coordinate, X. Accordingly, the axial derivative, $\partial\phi/\partial X$, remains continuous, while the radial and angular derivatives, $\partial^2\phi/\partial R^2$ and $\partial^2\phi/\partial\theta^2$, are replaced by finite difference formulations using values of unknown quantities on the same line and on neighboring lines, Figs. 2 and 3. Hence, this simple mathematical concept generates a system of ordinary differential equations of the first order where the dependent variables are described along each line in terms of a single independent variable, X. It may, therefore, be readily solved numerically employing a standard Runge–Kutta algorithm using the finite difference method. The partial differential equations for G^*, equation (14), can be discretized into an associated system of algebraic equations. Therefore, this system is carried out at each axial station, X, using

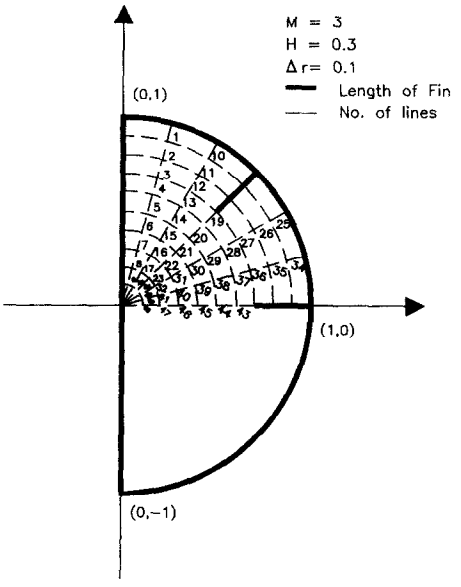

FIG. 2. Coordinate system for semicircular duct with $M = 3$ and $H = 0.3$.

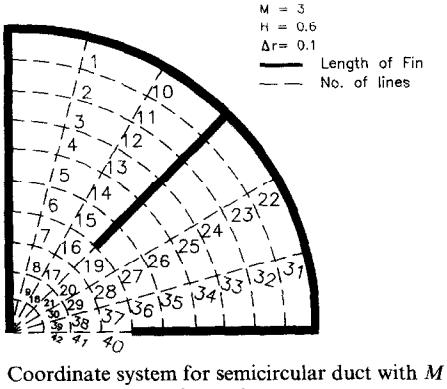

FIG. 3. Coordinate system for semicircular duct with $M = 7$ and $H = 0.6$.

an adaptation of the Gaussian elimination algorithm for the numerical determination of G^* at each cross section.

DISCUSSION OF RESULTS

The problem investigated in this paper deals with combined radiative and forced convection heat transfer in the entrance region of a semicircular duct with longitudinal internal fins. The mean bulk temperature, ϕ_b, equation (17), and the total Nusselt number, equation (19), are computed numerically using the MOL and MOM. The problem contains several parameters: optical thickness, τ_b; radiation–conduction, N; wall emissivity, ε_w; number of fins, M; and relative fin height, H. Numerical solutions were generated for a variety of combinations for the above-mentioned parameters. All computations were conducted on a micro VAX 8800. These computations are illustrated in Figs. 4–9.

To ensure the accuracy of the numerical solution, an independent grid size test has also been conducted in this study. Table 1 depicts the results of this test for different grid sizes. The number of fins, the relative fin height, wall emissivity, optical thickness, and conduction–radiation parameters in this test are $M = 3$, $H = 0.6$, $\varepsilon_w = 1.0$, $\tau_b = 5.0$, and $N = 0$, 1.0, 3.0, respectively. Inspection of the data indicates that almost identical results for the Nusselt number can be obtained with the number of lines specified in this table. Therefore, the smaller grid size is mainly used throughout this study when computing the Nusselt number.

In order to prove the validity of the proposed methodology, numerical solutions for a thermal entrance

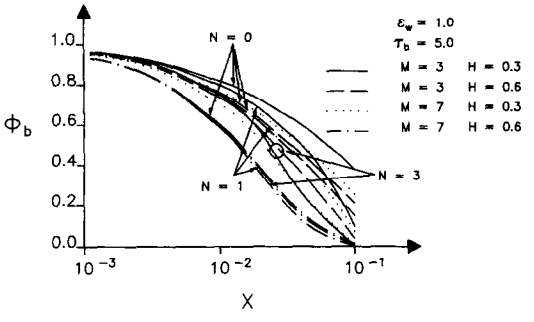

FIG. 4. Effects of conduction–radiation parameter, number of fins, relative fin heights on mean bulk temperature.

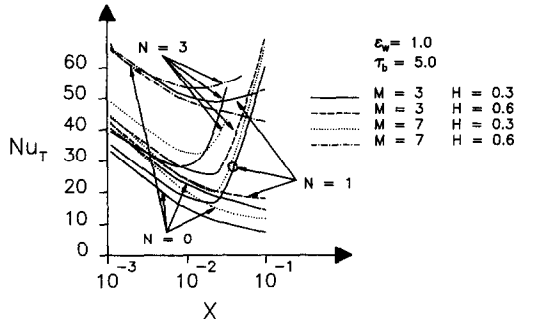

FIG. 5. Effects of conduction–radiation parameter, number of fins, and relative fin heights on the total Nusselt number.

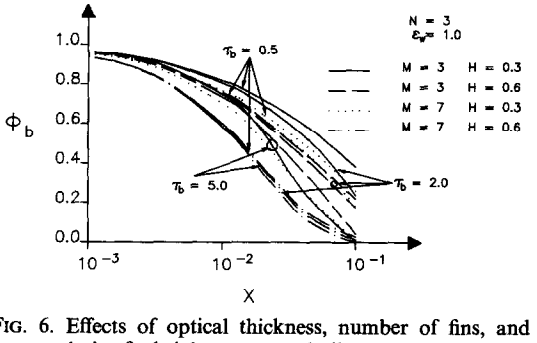

FIG. 6. Effects of optical thickness, number of fins, and relative fin heights on mean bulk temperature.

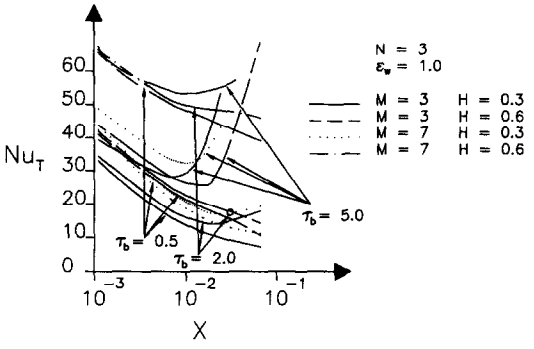

FIG. 7. Effects of optical thickness, number of fins, and relative fin heights on total Nusselt number.

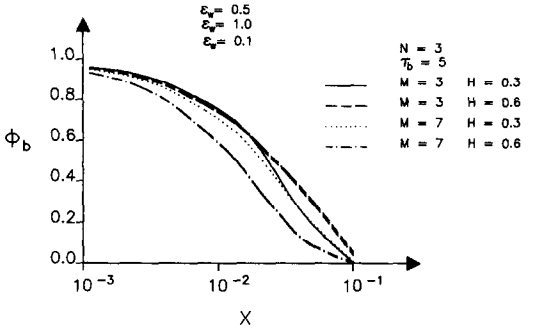

FIG. 8. Effects of wall emissivity, number of fins, and relative fin heights on the mean bulk temperature.

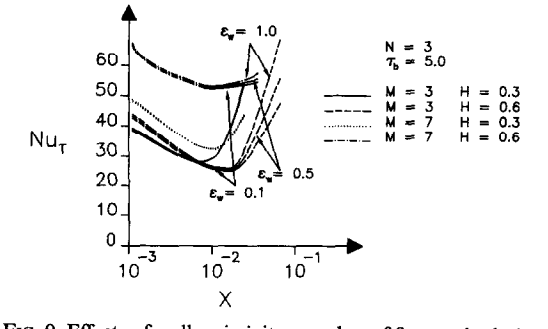

FIG. 9. Effects of wall emissivity, number of fins, and relative fin heights on the total Nusselt number.

Table 1. Effects of the grid size on the local Nusselt number for $M = 3$, $H = 0.6$, $\varepsilon_w = 1.0$, $\tau_b = 5.0$

		$N = 0$		$N = 1$		$N = 3$	
		Number of lines					
		78	96	78	96	78	96
$1/X$	X	$Nu_{x,T}$					
1000	0.00112	40.26636	40.39857	41.18594	41.34494	43.04618	43.25586
200	0.00485	27.51973	27.73492	28.68325	28.90509	31.10324	31.34966
180	0.00560	26.38192	26.54395	27.58617	27.75654	30.10766	30.28743
160	0.00635	25.45135	25.55182	26.69968	26.80737	29.32473	29.43640
120	0.00821	23.73195	23.68378	25.09274	25.03304	27.99566	27.90842
100	0.01000	22.53957	22.41231	24.01942	23.85207	27.22100	26.97054
80	0.01232	21.49737	21.18621	23.12299	22.75927	26.69784	26.21101
60	0.01680	20.08234	19.61297	22.00215	21.44407	26.36026	25.56293
50	0.02016	19.34419	18.82086	21.48791	20.84562	26.47397	25.50075
40	0.02501	18.55629	18.00842	21.03577	20.32712	27.01481	25.86346
30	0.03322	17.66386	17.14091	20.75389	20.01641	28.76411	27.8443
20	0.05000	16.61716	16.18327	21.20759	20.45445	35.93944	33.74314
10	0.10000	14.30264	14.10567	27.12895	25.62045		
9	0.11123	13.63986	13.50776	30.18234	28.11092		

region, absent of radiation ($N = 0$), but with internal longitudinal fins have been carried out. The values of Nu_T are plotted vs the axial position and compared with the results of ref. [24], as shown in Fig. 4. Inspection of the curves in this figure indicates very close agreement with the above-mentioned reference which further validates the proposed methodology.

Figures 4 and 5 depict the axial variation of the mean bulk temperature and total Nusselt number with wall emissivity of $\varepsilon_w = 1.0$; optical thickness of $\tau_b = 5.0$; number of fins, $M = 3$ and 7; relative fin heights of $H = 0.3$ and 0.6 for radiation–conduction parameters of $N = 0$, 1 and 3.0. Figure 4 indicates that the mixed mean temperature increases very rapidly with a decrease of the radiation–conduction parameter. The curves for $N = 0$ in this figure relate to pure forced convection. Comparison of curves for $N = 0$ with those given in ref. [24] indicates excellent agreement which further validates the proposed methodology. In addition, it is observed that increasing the number of fins and relative fin height, increases the development of the mean bulk temperature. Figure 5 indicates that the total Nusselt number increases as both the radiation–conduction parameter and the number of fins increases. In fact, it is seen that the total Nusselt number attains a minimum, and beyond that point, increases dramatically. To explain this phenomenon, as the gas passes through the duct, the position of the minimum Nusselt number shifts toward the inlet of the channel, indicating a more rapid development in the fluid, after which radiation is the dominant factor controlling the total Nusselt number.

Figures 6 and 7 represent the variation of the axial mean bulk temperature and the total Nusselt number with wall emissivity of $\varepsilon_w = 1.0$; a radiation–conduction parameter of $N = 3$ for optical thicknesses of $\tau_b = 0.5$, 2.0, and 5.0; number of fins, $M = 3$ and 7; and relative fin height of $H = 0.3$ and 0.6. It is observed that at the entrance region of the semicircular duct, there is basically no deviation in the mean bulk temperature at different optical thicknesses. Additionally, increasing the number of fins in the same region would increase the surface area enhancing convective heat transfer. This can be explained by the fact that forced convection is dominant at the entrance region of the semicircular duct. However, as the gas passes through the duct, a significant deviation is observed in the mean bulk temperature as the optical thickness, number of fins and relative fin heights increase. Obviously, this is due to the fact that the dominant term is radiative at the end of the channel. Figure 7 represents the total Nusselt number for the same conditions, and the same behavior can be observed. In fact, inspection of the curves in this figure indicates that the total Nusselt number is highest at $\tau_b = 5.0$, $M = 7$, and $H = 0.6$. Additionally, full thermal development is never reached in these figures in the presence of radiation.

Figures 8 and 9 illustrate the mean bulk temperature and total Nusselt number with radiation–conduction, $N = 3$; optical thickness of $\tau_b = 5$; number of fins, $M = 3$ and 7; and relative fin heights of $H = 0.3$ and 0.6 for wall emissivities of $\varepsilon_w = 0.1$, 0.5, and 1.0. Figure 8 indicates that the mean bulk temperature is unaffected at the entrance region of the semicircular duct with wall emissivity. However, in the region of $10^{-2} < X < 10^{-1}$, the mean bulk temperature decreases as the number of fins, fin heights, and wall emissivities are increased. Figure 9 indicates the same behavior as explained previously in Figs. 5 and 7. However, it is observed that increasing wall emissivity enhances the total Nusselt number dramatically.

SUMMARY AND CONCLUSIONS

The combination of radiation and forced convection has been examined in this paper for the flow of an absorbing–emitting gas in an isothermal duct of

semicircular cross section with longitudinal internal fins. The significant role played by radiation and internal fins in the thermal entrance region has been successfully represented by the MOM and the MOL. The nodes have been carefully placed along the surfaces to avoid the usual difficulties with irregular boundaries. The use of coarse grids in the cross section of the duct yields a relatively small system of first-order ordinary differential equations. Hence, this system can readily be solved by either analytical or numerical techniques. The effects of the different physical parameters were systematically studied. The following conclusions were obtained.

(1) The interaction of radiation with forced convection and fins increases the convective heat flux at the wall and, in general, results in an augmentation of the heat transfer process.

(2) Radiation–conduction, N, optical thickness, τ_b, and wall emissivity, ε_w, are the major parameters affecting radiation heat transfer.

(3) The total Nusselt number for the semicircular duct attains a minimum value at certain downstream locations, and beyond these points, Nu_T increases again. As N increases, the minimum points of Nu_T shift toward the entrance direction.

(4) Increasing the number of fins and relative fin heights, increases the Nusselt number accordingly, and thus, delays the development of the local Nusselt number in the entrance region of the duct.

Acknowledgement—The results presented in this paper were obtained in the course of research sponsored by the Department of Energy under subcontract No. 19X-SE133V.

REFERENCES

1. E. R. G. Eckert, R. G. Goldstein, E. Pfender, W. E. Ibele, S. V. Patankar, S. W. Ramsey, T. W. Simon, N. A. Decker, T. H. Kuehn, H. O. Lee and S. L. Girshick, Heat transfer—a review of the 1986 literature, *Int. J. Heat Mass Transfer* **30,** 2449–2523 (1987).
2. E. R. G. Eckert, R. G. Goldstein, E. Pfender, W. E. Ibele, S. V. Patankar, S. W. Ramsey, T. W. Simon, N. A. Decker, T. H. Kuehn, H. O. Lee and S. L. Girshick, Heat transfer—a review of the 1987 literature, *Int. J. Heat Mass Transfer* **31,** 2401–2488 (1988).
3. E. R. G. Eckert, R. G. Goldstein, E. Pfender, W. E. Ibele, S. V. Patankar, S. W. Ramsey, T. W. Simon, N. A. Decker, T. H. Kuehn, H. O. Lee and S. L. Girshick, Heat transfer—a review of the 1988 literature, *Int. J. Heat Mass Transfer* **32,** 2211–2280 (1989).
4. S. Kakac, R. K. Shah and W. Aung, *Handbook of Single-phase Convective Heat Transfer*. Wiley/Interscience, New York (1987).
5. R. K. Shah and A. L. London, *Laminar Flow Forced Convection in Ducts*. Academic Press, New York (1978).
6. R. I. Soloukhin and O. G. Martynenko, Heat and mass transfer bibliography—Soviet literature, *Int. J. Heat Mass Transfer* **26,** 1771–1781 (1983).
7. O. G. Martynenko, Heat and mass transfer bibliography—Soviet literature, *Int. J. Heat Mass Transfer* **31,** 2489–2503 (1988).
8. B. E. Pearce and A. Emery, Heat transfer by thermal radiation and forced convection in an absorbing fluid in the entry region of a pipe, *J. Heat Transfer* **92,** 221–230 (1970).
9. R. Echigo, S. Hasegawa and K. Kinamuto, Composite heat transfer in a pipe with thermal radiation in a flowing medium, *Int. J. Heat Mass Transfer* **18,** 1149–1159 (1975).
10. Y. Yener and T. M. I. Fong, Radiation and forced convection interaction in thermally developing laminar flow through a circular pipe, *Proc. 8th Int. Heat Transfer Conf.*, Vol. 2, pp. 785–790 (1986).
11. M. H. Hu and Y. P. Chang, Optimization of finned tubes for heat transfer in laminar flow, *J. Heat Transfer* **95,** 332–338 (1973).
12. K. Nandakumar and J. H. Masliyah, Fully developed viscous flow in internally finned tubes, *Chem. Engng J.* **10,** 113–120 (1975).
13. H. M. Soliman and A. Feingold, Analysis of fully developed laminar flow in internally finned tubes, *Chem. Engng J.* **14,** 119–128 (1977).
14. H. M. Soliman and A. Feingold, Analysis of heat transfer in internally finned tubes under laminar flow condition, *Proc. 6th Int. Heat Transfer Conf.*, Vol. 2, pp. 571–576 (1978).
15. H. M. Soliman, T. S. Chau and A. C. Trupp, Analysis of laminar heat transfer in internally finned tubes with uniform outside wall temperature, *J. Heat Transfer* **102,** 598–604 (1980).
16. C. Prakash and S. V. Patankar, Combined free and forced convection in vertical tubes with radial internal fins, *J. Heat Transfer* **103,** 566–572 (1981).
17. C. Prakash and Y. D. Liu, Analysis of laminar flow and heat transfer in the entrance region of an internally finned circular duct, *J. Heat Transfer* **107,** 84–91 (1985).
18. I. M. Rustum and H. M. Soliman, Numerical analysis of laminar forced convection in the entrance region of tubes with longitudinal internal fins, *J. Heat Transfer* **110,** 310–313 (1988).
19. I. M. Rustum and H. M. Soliman, Experimental investigation of laminar mixed convection in tubes with longitudinal internal fins, *J. Heat Transfer* **110,** 366–372 (1988).
20. A. Campo, Variational technique applied to radiative–convective fins with steady and unsteady conditions, *Wärme- und Stoffübertr.* **9,** 139–144 (1976).
21. M. N. Özisik, *Radiative Heat Transfer*. Wiley, New York (1973).
22. D. A. Liskovets, The method of lines (review), *Differential Equation* **1,** 1308–1323 (1965).
23. H. A. Carnahan and J. O. Wilkes, *Applied Numerical Methods*. Wiley, New York (1969).
24. H. Y. Zhang, M. A. Ebadian and A. Campo, Flow and thermal analysis of laminar forced convection in the entrance region of semi-circular duct with longitudinal internal fins, 1990 AIAA/ASME Thermophysics Heat Transfer Conf., Numerical Heat Transfer, HTD-130, pp. 53–60 (1990).
25. P. Wilbulswas, Laminar flow heat transfer in non-circular ducts, Ph.D. Thesis, London University, London (1966).

TRANSFERT THERMIQUE CONVECTIF-RADIATIF DANS LA REGION D'ENTREE D'UN TUBE SEMI-CIRCULAIRE AVEC DES AILETTES INTERNES LONGITUDINALES

Résumé—On analyse le transfert permanent de convection forcée laminaire avec rayonnement dans la région d'entrée d'un tube semi-circulaire aileté intérieurement. Les ailettes sont continues et longitudinales avec une épaisseur nulle. La condition imposée sur le tube est celle de température uniforme à la fois axialement et sur la périphérie. L'équation d'énergie tridimensionnelle est discrétisée et résolue numériquement par la méthode des lignes (MOL). La méthode de la quantité de mouvement (MOM) est employée pour considérer la contribution du rayonnement qui modélise le rayonnement dans l'équation aux dérivées partielles, au lieu de l'équation intégro-différentielle. Les équations résultantes sont calculées numériquement en utilisant la subroutine Runge–Kutta. On discute l'effet de cinq paramètres principaux sur le comportement dans la région d'entrée du tube : rayonnement–conduction N, épaisseur optique τ_b, émissivité de la paroi ε_w, nombre d'ailettes M, et rapport de la hauteur de l'ailette au rayon du tube H. Les variations de la température moyenne à coeur et des nombres de Nusselt globaux montrent que le transfert thermique est augmenté dans cette géométrie à la fois par le rayonnement et par les ailettes.

WÄRMEÜBERTRAGUNG DURCH KONVEKTION UND STRAHLUNG IM THERMISCHEN EINLAUFGEBIET EINES HALBKREISFÖRMIGEN KANALS MIT INNEREN LÄNGSRIPPEN

Zusammenfassung—In der vorliegenden Arbeit wird die Wärmeübertragung durch stationäre laminare erzwungene Konvektion und Strahlung im Einlaufbereich eines innenberippten, halbkreisförmigen Kanals untersucht. Die Rippen, mit der Dicke Null, sind zusammenhängend und in Längsrichtung angebracht. Als thermische Randbedingung wird dem halbkreisförmigen Kanal in axialer und in Umfangsrichtung eine gleichförmige Temperatur aufgeprägt. Die dreidimensionale Energiegleichung wird diskretisiert und nach der Linienmethode (MOL) numerisch gelöst. Zur Berücksichtigung des Strahlungsbeitrags wird die Momentenmethode (MOM) angewandt, bei der die Strahlung in der partiellen Differentialgleichung anstatt der partiellen Integro-Differentialgleichung modellmäßig erfaßt wird. Die resultierenden Gleichungen, die auf einem groben Gitter basieren, werden mit einem Runge–Kutta Unterprogramm berechnet. Der Einfluß von 5 Hauptparametern auf das thermische Verhalten im Einlaufgebiet des halbkreisförmigen Kanals wird untersucht: N für Strahlung–Leitung; τ_b für die optische Dicke; ε_w für die Wandemissivität; M für die Zahl der Rippen und H für das Verhältnis aus Rippenhöhe und Kanalradius. Die Veränderungen der mittleren Fluidtemperatur und der Nusselt-Zahl zeigen, daß der Wärmeübergang bei dieser geometrischen Anordnung sowohl durch die thermische Strahlung als auch durch die Berippung verbessert wird.

КОНВЕКТИВНО–РАДИАЦИОННЫЙ ТЕПЛОПЕРЕНОС ВО ВХОДНОЙ ОБЛАСТИ В ПОЛУКРУГЛЫЙ КАНАЛ С НАПРАВЛЕННЫМИ ПО ТЕЧЕНИЮ ВНУТРЕННИМИ РЕБРАМИ

Аннотация—Анализируются стационарная ламинарная вынужденная конвекция и радиационный теплоперенос во входной области полукруглого канала с ребрами. Ребра являются сплошными, продольно направленными и имеют нулевую толщину. На оси и периферии канала поддерживается постоянная температура. Трехмерное уравнение энергии решается численным методом. Вклад излучения описывается не интегро-дифференциальным, а дифференциальным уравнением в частных производных. Результирующие уравнеия решаются численно методом Рунге–Кутта. Обсуждается влияние на тепловой режим во входной области канала пяти основных параметров: роли переноса энергии излучением по сравнению с переносом теплопроводностью N, оптической толщины τ_b, поглощательной способности стенки ε_w, числа ребер M, отношения высоты ребра к ралиусу канала H. Изменения среднемассовой температуры и числе Нуссельта показывают, что в рассматриваемой геометрии теплоперенос усиливается как за счет теплового излучения, так и за счет ребер.